Observation and Hydrodynamic Simulation of Tidal Current and Seawater Exchange in the Kesennuma Bay, Northeastern Japan

Reo SHIBASAKI[1], Tetsuya SHINTANI[2], Keitaro FUKUSHIMA[3], Masayuki KOBAYASHI[4] and Katsuhide YOKOYAMA[5]

[1] Member of JSCE, Graduate Student, Dept. of Civil and Environmental Eng., Tokyo Metropolitan University
(1-1, Minami-Osawa, Hachioji-shi, Tokyo 192-0397, Japan)
E-mail: shibasaki-reo@ed.tmu.ac.jp
[2] Member of JSCE, Assistant Professor, Dept. of Civil and Environmental Eng., Tokyo Metropolitan University
(1-1, Minami-Osawa, Hachioji-Shi, Tokyo 192-0397, Japan)
E-mail: shintani@tmu.ac.jp
[3] Member of JSCE, Researcher, Center for Ecol. Res., Kyoto University
(2-509-3, Hirano, Otsu, Shiga 520-2113, Japan)
E-mail: ktaro.f@gmail.com
[4] Member of JSCE, Yachiyo Engineering CO., LTD.
(CS Tower, 5-20-8, Asakusabashi, Taito-ku, Tokyo 111-8648, Japan)
E-mail: msy-kobayashi@yachiyo-eng.co.jp
[5] Member of JSCE, Professor, Dept. of Civil and Environmental Eng., Tokyo Metropolitan University
(1-1, Minami-Osawa, Hachioji-shi, Tokyo 192-0397, Japan)
E-mail: k-yoko@tmu.ac.jp

We observed the seawater flow pattern during the ebb and flood tide in the Kesennuma Bay, northeastern Japan, using towing and bottom-mounted ADCPs. We also simulated the flow pattern with the hydrodynamics simulation model Fantom-Refined in order to elucidate the characteristics of water current in relation to the topography. The observed data indicated that the eastern bay had a large flow rate compared to the western bay. It was also found that topographical condition strongly influenced the direction of the tide-induced flow. Numerical simulation result indicated that the ebb current at a depth of 5 m was found to be weakened around the Okawa River mouth; in the northern part of the western bay, and the flow was prevailing through the narrow channel called Oshima-Seto to east. During the flood tide, the inward water flow from the Pacific Ocean to both the eastern and the western bay was dominant, but the current was weakened and reversed in the middle region of the western bay. This flow pattern should be caused mainly by asymmetricity of the depth between the eastern and the western part of the Kesennuma Bay.

Key Words : *Kesennuma Bay, semi-closed bay, ADCP, hydrodynamic simulation, Fantom-Refined*

1. INTRODUCTION

A semi-closed bay is characterized by its calm and nutrient-rich environment that allows high-quality fisheries and aquaculture. There is also a risk that excess nutrient input from a river would result in environmental deterioration such as eutrophication and harmful algal blooms[1)]. It is necessary to understand seawater current inside the bay and its exchange between the ocean and bay for the efficient management of the aquatic environment since they are one of the most important factors controlling the transport and diffusion of nutrients and phytoplankton.

The Sanriku coast, which is located in northeastern Japan, is a fertile area for oysters and scallops cultivation because of its complex topographical features and presence of Oyashio current[2,3)]. The Kesennuma Bay, a part of the Sanriku ria coast, is one of the most popular fields for aquaculture in Japan. However, few studies were conducted in the area to assess the dynamics of tidal current interacting with the topography[4,5)], so factors regulating current pattern are still unclear in this bay. The aim of this study is the elucidation of the major factors determining seawater current and exchange in the bay with the aid of in-situ observation data and numerical simulations.

2. METHODOLOGY

(1) Study Area

Kesennuma Bay is approximately 8 km wide in an east-west direction and 10 km long in a north-south direction, which is located in the eastern Miyagi Prefecture, Japan (**Fig. 1**). There is the Oshima Island in the center of the bay, separating the bay into the eastern and western part. Based on the marine chart (W1099, measured on March, 2015) published by the Japan Hydrographic Association, the water depths are approximately 10 m and 30 m in the western bay and eastern bay, respectively. Okawa River has the largest basin area among the rivers flowing into the Kesennuma Bay (168 km^2) and its mouth locates at the western bay. Kesennuma-Port and the central part of Kesennuma city is located in the most inner part of the western bay. In the northern part of the Oshima Island, there is a meandering narrow channel called "Oshima-Seto" connecting the western and eastern bay, which has the complicated submarine topography.

Since some part of seafloor topography in this narrow channel was not measured accurately by the marine chart, we refined it with our own measuring data. On December 12, 2016, seafloor topography measurement was carried out along the 22 lines across the Oshima-Seto (**Fig. 2**) using an echo-sounder (LCX-27C, Lowrance). These line data were used as inputs for iRIC (International River Inter-face Cooperative) software to obtain interpolated topography in longitudinal direction. As a result of this survey, the channel of average depth 35 m (41 m at maximum) appeared along the Oshima-Seto.

(2) Velocity Measurement

Velocity measurement of 8 lines was carried out two times on June 19, 2015, in order to understand the flow pattern of the tide-induced flow during spring tide (**Fig. 2**). Towing ADCP (Acoustic Doppler Current Profiler, WorkHorse Monitor 600 kHz, Teledyne RD Instruments) in bottom tracking mode was used. The ADCP was attached to the boat and run at the speed of 6 to 9 km h^{-1}. Measurement conditions of the velocity were as follows; depth cell size was 0.5 m, surface blank was 1.60 m, the numbers of bottom and water pings were both 5, and standard deviation was 5.76 cm s^{-1}. In general, obtained data accuracy depends on the number of pings, but it takes much time so it was difficult to obtain a lot of pings at each line while moving. In our observation, synchronicity in the measurement is considered to be more important than data quality for the wide-spread grasp of current velocity.

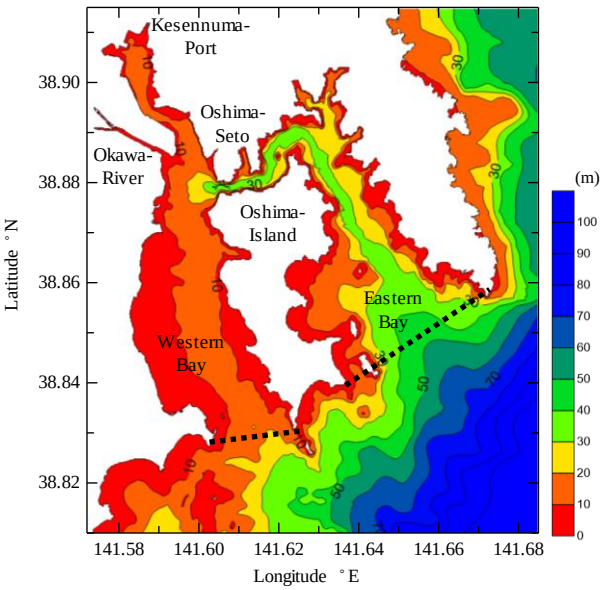

Fig. 1 Study area. Dotted lines indicate the bay mouth.

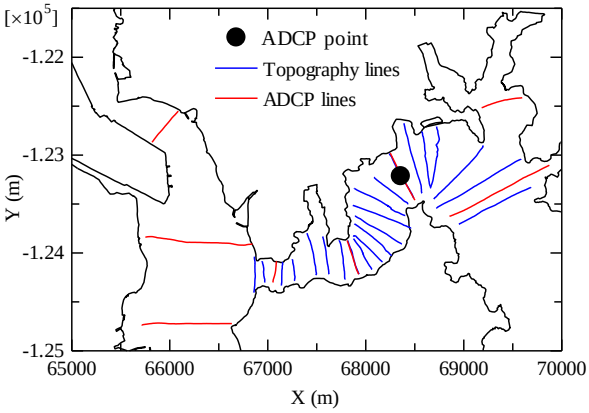

Fig. 2 Location of data measurement

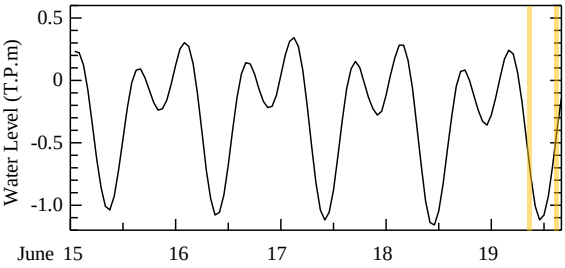

Fig. 3 Tidal level at Ayukawa-Port during the period for the numerical simulation. Orange shaded portion indicates the measurement period using towing ADCP.

First round was done from 7:52 am (UTC+9) to 9:15 am during ebb tide, and second round was done from 2:04 pm to 3:20 pm during flood tide (**Fig. 3**).

Vertical profile of current velocity had been continuously acquired at the center of Oshima-Seto simultaneously using bottom mounted ADCP (WorkHorse Sentinel 600 kHz, Teledyne RD Instruments) from January 17 to June 19, 2015. Depth cell size, surface blank, standard deviation, and time interval are 0.5 m, 3.0 m, 1.29 cm s^{-1}, and 10 minutes, respectively[5].

(3) Numerical Simulation

The tidal current pattern was reproduced using a three-dimensional hydrodynamic simulator, Fantom-Refined[6]. The basic equations utilized in the model were the equation of continuity and three-dimensional Navier-Stokes equations with incompressible and Boussinesq approximations. The equations were discretized based on a collocated finite volume method. Temporal derivertives were discretized using the second-order Adams-Bashforth method for explicit terms and also second order theta-method for semi-implicit terms, while the advection terms were discretized by the third-order ULTIMATE QUICKEST scheme. Detailed information are given in Shintani (2017)[6]. Although the simulator can solve hydrostatic and non-hydrostatic problems, only hydrostatic components of the simulator was used in this study. For the calculation of vertical eddy viscosity and diffusion coefficients, GLS turbulence closure model was used[7].

In this study, the horizontal grid size was 20 m in the inner bay and narrow channel, and gradually increased from 40 m to 640 m and 1280 m near open ocean boundary to shorten the computation time (**Fig. 4**). Vertical grid size was 0.2 m at surface and increased up to 20 m at bottom. Total number of vertical cells is 49. Consequently, the total number of cells during high tide was about 290,000 cells. The time step was set to 5 sec through the computation.

Initial conditions were based on measured vertical temperature distribution (from 17 °C at the surface to 11 °C at the bottom) and constant salinity (33.65 psu at the bottom) on June 18, 2015, at a point where the bottom-mounted ADCP was installed. As for the boundary conditions, tidal level and fresh water discharge were specified at the open boundary and river upstream, respectively, while wind stress and heat fluxes were applied to the surface boundary. Tidal level was given at around 10 km offshore from two open boundary, at south and east sides, which was obtained from Japan Meteorological Agency (JMA) observed in Ayukawa-Port (38º18'N, 141º30'E). Salinity in open boundary was given as the same value as the initial condition (33.65 psu). Weather data (wind, temperature, humidity, solar radiation, atmospheric pressure, rainfall and cloud cover) were given uniformly. These data were from JMA observed in Kesennuma (38º54'N, 141º33'E), Ofunato (39º04'N, 141º43'E) and Sendai (38º16'N, 140º54'E). In performing numerical simulation, it is necessary to convert wind data obtained in inland areas to offshore wind. Arakawa et al. (2007) proposed a method to estimate the offshore wind using a 3-dimentional non-linear wind prediction model, and evaluated the wind speed ratio between the inland

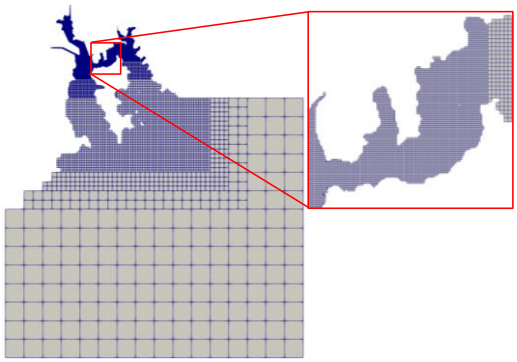

Fig.4 Grid resolution for the simulation.

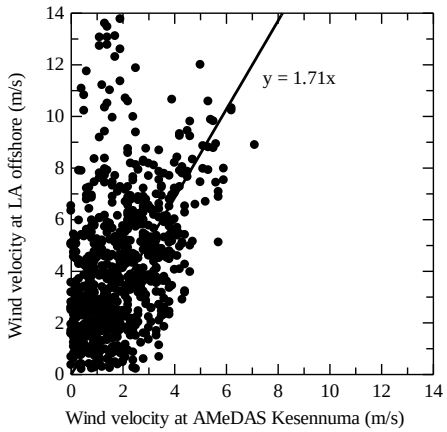

Fig. 5 The relationship between inland wind velocity at Kesennuma weather station and offshore wind velocity obtained from Local Analysis performed by JMA. The correlation was statistically significant ($P< 0.01$).

wind and the offshore wind as 1.5[8]. In our study, we used the wind data of Local Analysis (LA), which is a product of objective analysis performed by JMA and utilized as an initial condition for the Local Forecast Model (LFM). The LA dataset has a horizontal resolution of 5 km, and a temporal resolution of 1 hour. A comparison of LA data with inland observation data in the Kesennuma weather station reveals that offshore wind velocity was about 1.71 times higher than inland one (**Fig. 5**). Large variations in offshore wind velocity at less than 2 m s^{-1} of inland wind velocity were rarely detected because of a low atmospheric pressure area developed in the ocean. The distribution of wind direction was almost same between them. Therefore, we input offshore wind velocity into the model by multiplying the inland wind data by 1.71.

Okawa River discharge was given at the cell of the upstream end in the computational domain. The discharge data was calculated by the H-Q equation using water level observed 5 km upstream from the river mouth. Discharge from other several small rivers was estimated by multiplied Okawa River discharge by the rate of each catchment area. Numerical simulation was conducted to estimate the surface and flow fields in the bay from June 15 to 19 in 2015. Total rainfall during the period was 46 mm.

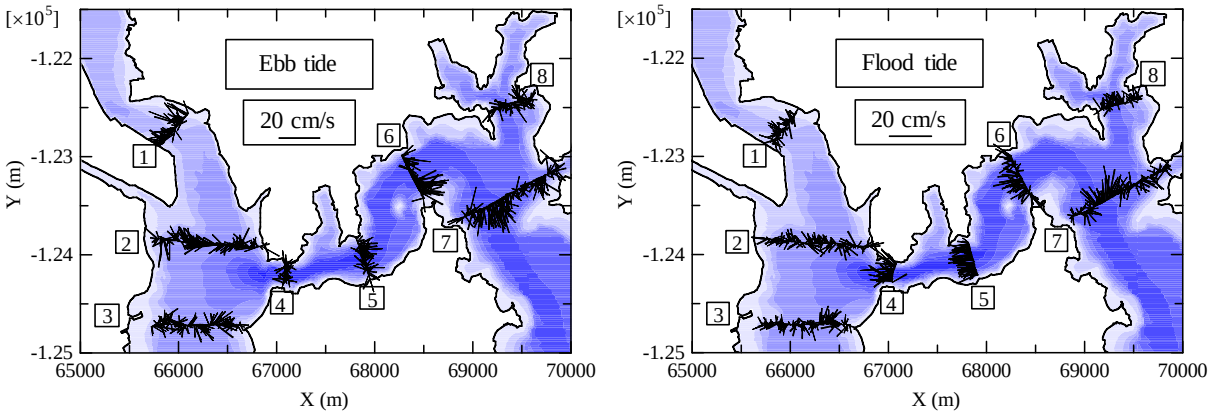

Fig. 6 Distribution of seawater velocity at a 5 m depth from the surface measured by towing ADCP.

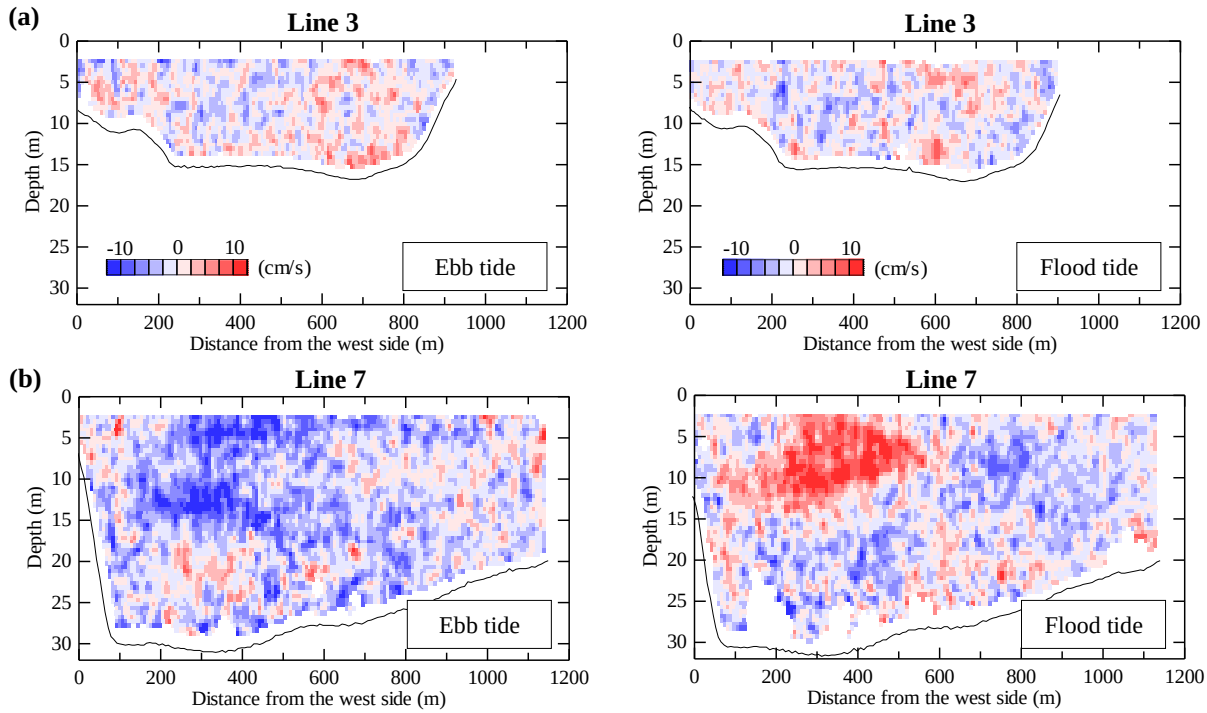

Fig. 7 Observed velocity of seawater current at a cross section (a) Line 3 and (b) Line 7 during the ebb tide (Left) and the flood tide (Right). The flow was directed perpendicularly to the measured lines and given the direction such that the flow direction of seawater from the line to the inner bay was positive (+), and the outflow direction was negative (-).

3. RESULTS AND DISCUSSION

(1) Observed Seawater Flow Velocity

The magnitude and direction of observed velocity at a depth of 5 m in 8 measured lines were shown in **Fig. 6**. The results showed that the seawater mainly flowed out from the eastern bay via the Oshima-Seto channel during the ebb tide. On the other hand, at the flood tide, the current was directed towards the mouth of the Okawa River estuary from the eastern bay via Oshima-Seto.

Fig. 7 shows the observed velocity of water current at the cross-sections of lines 3 and 7. The result indicated that the eastern bay had a large cross-section flow rate compared to the western bay. As the highest velocity was observed across the largest cross section (Line 7), it can be inferred that seawater flow was mainly generated in the eastern bay near the surface (< 15 m depth). In addition, beneath this layer, the direction of main flow was opposite. This two layer structure, of which boundary would be in a depth of 15 m, is likely caused by the difference of the maximum water depth between the eastern and western bay as previously reported in Yokoyama et al. (2016)[5].

Moreover, the flow direction opposite to the main flow was also observed in the east side of line 7 (**Fig. 7(b)**). It can be attributed to the coastal topography that the channel just to the south of line 7 becomes narrow in width along the flow. This condition might have been generated as a compensational flow of the main stream near the surface. Thus, in Kesennuma Bay, it was found that complicated topography severely influenced the transport of the seawater inside the Kesennuma Bay.

(2) Numerical Simulation

Fig. 8 shows measured and computed results of the water level and velocity at depths of 5 m, 15 m, and 25 m at the point where the bottom mounted ADCP was installed. Positive value indicates the velocity toward east-north-east. The amplitude and period of the variations in velocity indicate the similar trend between measured and computed values (**Fig. 8**). However, a large gap was seen between them at a depth of 5 m on 15-16 June. This may be partly due to the strong local wind generated by the specific climate condition and/or the effect of river inflow during heavy rainfall. Further improvement should be necessary for more accurate predictions. Overall, as the computed values showed almost good agreements with observed ones, the simulated results of the spatial and vertical distribution of seawater current in the entire Kesennuma Bay would be reliable for discussing the flow structure.

From **Fig. 9(a)**, the ebb current at a depth of 5 m was found to be weakened around the mouth of the Okawa River; in the northern part of the western bay (X = 66000 – 67000 m, Y = -1.235×10^5 m), and the flow was prevailing through the Oshima-Seto to the eastern bay. On the other hand, during the flood tide, the inward water flow from the Pacific Ocean to both the eastern and the western bay was dominant, but the current was weakened and reversed in the middle region of the western bay (X = 66000 – 68000 m, Y = -1.26 – -1.25×10^5 m, **Fig. 9(b)**), mainly because of asymmetricity of the average depth between the eastern and the western bay.

It is also possible to infer that during ebb tide, the upper layer was strongly affected by the barotropic forcing while in the deeper layer the seawater flowed in the reverse direction as observed in line 7 (**Fig. 7(b)**) and at the point where the ADCP is installed (**Fig. 8**). In contrast, during the flood tide, although

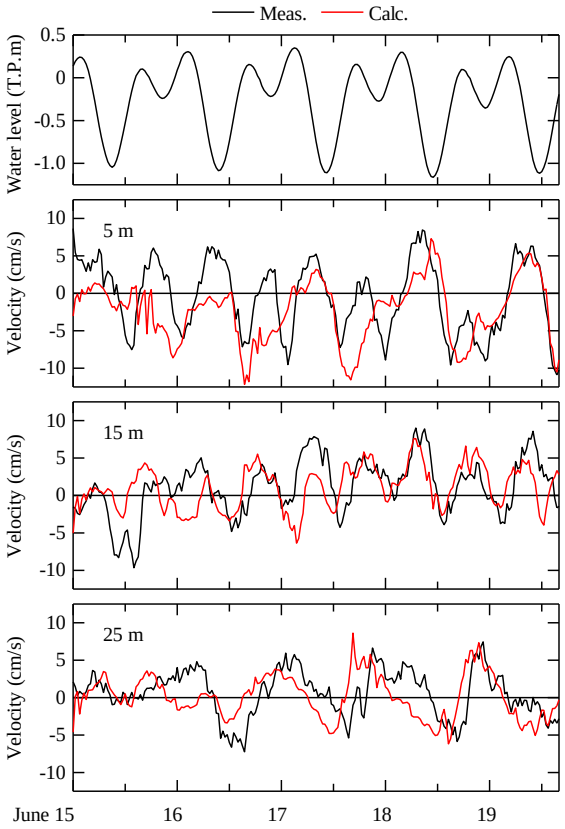

Fig. 8 The comparison of temporary variation of the flow velocity between the measured values (black line) and the values calculated by Fantom-refined (red line) at a depth of 5, 15, and 25 m accompanied with observed water level at a point where the ADCP was installed.

the inflow from the eastern bay is strongly directed towards the eastern part of the Okawa River mouth via the Oshima Seto, the velocity was weakened and its direction was became complicated around the Okawa River mouth. These results indicate that in the inner part of Kesennuma Bay (X = 65000 – 66000 m, Y = -1.23 – -1.21×10^5 m, **Fig. 9**), tidal current would be weakened significantly and it would make the rate of seawater exchange lowered.

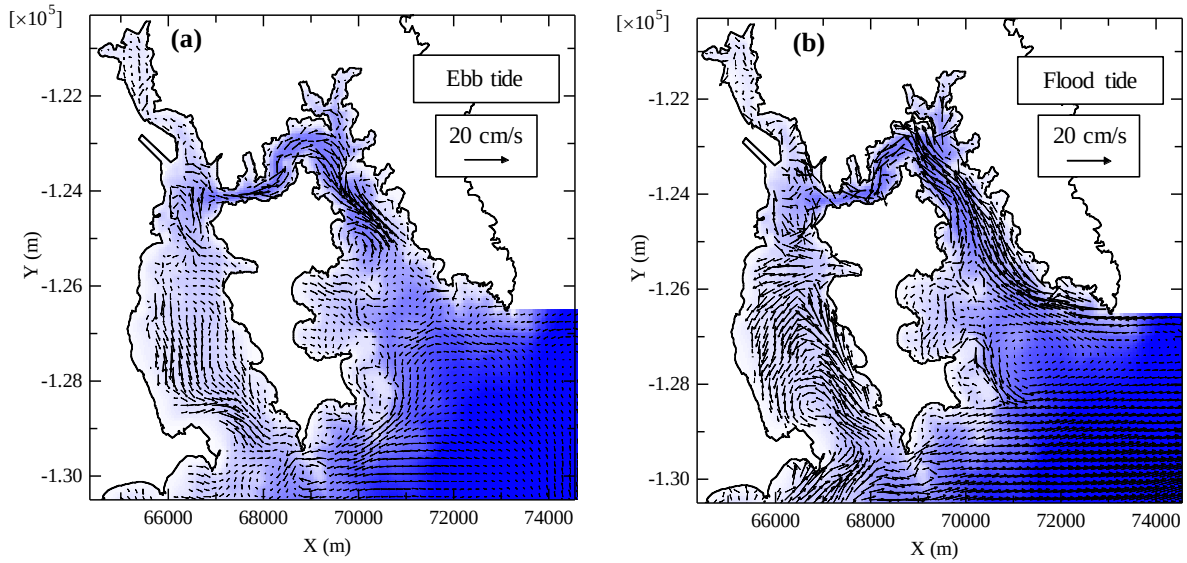

Fig. 9 Calculated velocity distribution during (a) ebb tide and (b) flood tide at a 5 m depth from the surface.

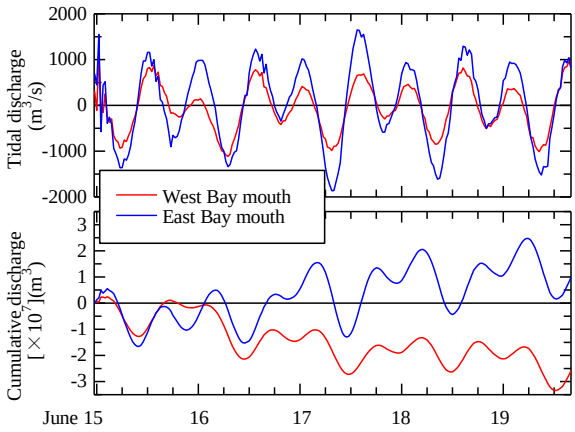

Fig. 10 Simulated result of a temporal variation of the (a) tidal current and (b) cumulative seawater movement during June 15 to 19, 2015, in a cross section of the western and eastern bay mouth. Positive value shows a direction from the Pacific Ocean to each bay.

Quantitative estimation of the discharge fluctuation was also determined in the boundary between the Pacific Ocean and the eastern and western bays (bay mouth; **Fig. 1**), based on the simulated results. There was a clear difference in temporal variation of tidal current and cumulative seawater movement between the eastern and western part of the Kesennuma Bay (**Fig. 10**). The rate of seawater exchange between the Pacific Ocean and the eastern bay was estimated more than 1000 m^3 s^{-1} during peak time, which was 1.5 times higher than that at the western bay. This result suggests that seawater exchange to the Pacific Ocean is mainly due to the tidal flow in the eastern bay rather than in the western bay. The cumulative seawater movement was landward in the eastern bay while it was seaward in the west bay. It also suggests that the prevailing current flow is likely counterclockwise from the eastern to the western bay via the Oshima-Seto channel. This might be attributed to the complex topography of the bay such that the eastern bay has the deeper seafloor and the wider baymouth than the western bay.

Seawater flowing in the upper layer of Kesennuma Bay may contain a high concentration of phytoplanktons and nutrients such as dissolved nitrogen and phosphorus, and therefore have greatly affected the aquaculture business all year around. In winter and spring, the direction of main flow becomes opposite to our study season and its velocity increases due to significant inflow of the Tsugaru warm current and the cold Oyashio current, respectively[5]. Therefore, it is necessary to consider the seasonality of seawater inflow from the Pacific Ocean for more accurate estimation of seawater dynamics within the Kesennuma Bay. Moreover, we will elucidate the characteristics of river water into the bay during heavy rainfall by conducting additional simulation and demonstrate its influence on aquaculture industry in the future study.

4. CONCLUSIONS

The field measurement and numerical simulation has been conducted to understand the current patterns in the entire Kesennuma Bay. The measured velocity field indicated the anti-symmetric flow between the eastern and western bays and the two-layer structure having opposite flow direction between upper and deeper layer in the eastern bay. These seawater flow characteristics played an important role in exchanging the sea water inside the bay. The computed results well reproduced the measured velocity field. Lastly, the mass flux inside the bay was estimated at two cross sections from numerical results. It was found that the seawater in the bay was mainly exchanged through the eastern bay.

ACKNOWLEDGEMENTS

This research was supported in part by the River Fund of the River Foundation, Japan, and JSPS KAKENHI grant number 25249068. We also thank Dr. M. Kajino of Meteorological Research Institute, JMA for the discussion of meteorological simulations, and Mr. M. Hatakeyama of NPO Mori-umi, and the members of the laboratory of Hydraulic Engineering, Tokyo Metropolitan University for the filed survey.

REFERENCES

1) Anderson, D.M., Glibert, P.M. and Burkholder, J.M.: Harmful algae blooms and eutrophication; Nutrient sources, composition, and consequences. *Estuaries*, Vol. 25, No. 4b, pp. 704-726, 2002.
2) Itoh, S., Kaneko, H., Ishizu, M., Yanagimoto, D., Okunishi, T., Nishigaki, H. and Tanaka, K.: Fine-scale structure and mixing across the front between the Tsugaru Warm and Oyashio Currents in summer along the Sanriku Coast, east of Japan. *J. Oceanogr.*, Vol. 72, pp. 23-37, 2016.
3) Natsuike, M., Nishitani, G., Yamada, Y., Yokoyama, K. and Yoshinaga, I.: The occurrences of toxic dinoflagellate *Alexandrium tamarense* around the Pacific coast of Eastern and Northern Japan after the Great East Japan Earthquake, *Gekkan Kaiyo*, Vol. 46, No. 12, pp. 62-71, 2014.
4) Yakita, K., Akimoto K., Takikawa K., Hokamura, T., Ueda, M., Yoshinaga, T., Ariyoshi, K. and Yoshioka, M.: Spacial distribution of suspended sediment with ADCP in the Kesennuma Bay Oshima Strait, *J. JSCE, Ser. B3(Ocean Eng.)*, Vol. 71, No. 2, pp. I_485-I_490, 2015.
5) Yokoyama, K., Natsuike M., Wako, Y. and Ohno, A.: Hydrodynamic flow and phytoplankton transportation in the narrow channel of the Kesennuma Bay, *J. JSCE, Ser. B2(Coastal Eng.)*, Vol.72, No. 2, pp. I_1387-I_1392, 2016.
6) Shintani, T. : An unstructured-cartesian hydrodynamic simulator with local mesh refinement technique, *J. JSCE, Ser., B1(Hydr. Eng.)*, Vol. 73, pp. 1-6, 2017.
7) Shintani, T. : Performance of GLS turbulence closure model implemented in 3D unstructured hydrodynamic simulator, *J. JSCE, Ser., B1(Hydr. Eng.)*, Vol. 60, 2016.
8) Arakawa, H. : Prediction of sea surface wind distribution with a three dimensional wind model, *J. JSCE, Ser. B2(Coastal Eng.)*, Vol. 54, pp. 131_135, 2007.

(Received May 24, 2018)